

Reactions of α -Nucleophiles with Alkyl Chlorides: Competition between S_N2 and E2 Mechanisms and the Gas-Phase α -Effect

Stephanie M. Villano, Nicole Eyet, W. Carl Lineberger, and Veronica M. Bierbaum*

JILA, University of Colorado and the National Institute of Standards and Technology, Boulder, Colorado 80309, and Department of Chemistry and Biochemistry, University of Colorado, Boulder, Colorado 80309

Received February 16, 2009; E-mail: veronica.bierbaum@colorado.edu

Abstract: Reaction rate constants and deuterium kinetic isotope effects for the reactions of BrO^- with RCl ($\text{R} = \text{methyl, ethyl, isopropyl, and } tert\text{-butyl}$) were measured using a tandem flowing afterglow-selected ion flow tube instrument. These results provide qualitative insight into the competition between two classical organic mechanisms, nucleophilic substitution (S_N2) and base-induced elimination (E2). As the extent of substitution in the neutral reactants increases, the kinetic isotope effects become increasingly more normal, consistent with the gradual onset of the E2 channel. These results are in excellent agreement with previously reported trends for the analogous reactions of ClO^- with RCl . [Villano et al. *J. Am. Chem. Soc.* **2006**, *128*, 728.] However, the reactions of BrO^- and ClO^- with methyl chloride, ethyl chloride, and isopropyl chloride were found to occur by an additional reaction pathway, which has not previously been reported. This reaction likely proceeds initially through a traditional S_N2 transition state, followed by an elimination step in the S_N2 product ion-dipole complex. Furthermore, the controversial α -nucleophilic character of these two anions and of the HO_2^- anion is examined. No enhanced reactivity is displayed. These results suggest that the α -effect is not due to an intrinsic property of the anion but instead due to a solvent effect.

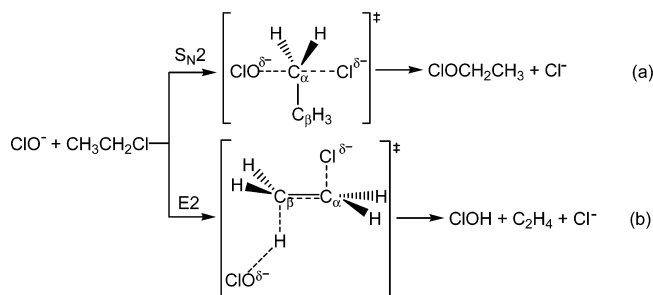
Introduction

Gas-phase ion-molecule studies provide a route to understanding the intrinsic factors that affect a reaction in an environment free from solvent. These studies, therefore, provide important insight into the role of the solvent in a given reaction. Several notable differences between the intrinsic gas-phase reactivity and the reactivity in solution have been observed.^{1–4} This work focuses on two important areas where solvent effects are significant: (1) the competition between nucleophilic substitution (S_N2) and base-induced elimination (E2) and (2) the α -effect or enhanced reactivity due to a lone pair of electrons that is adjacent to the nucleophilic center.

It has been shown, both experimentally⁵ and theoretically,⁶ that the gas-phase reaction of ClO^- with ethyl chloride proceeds through both an S_N2 and an E2 mechanism, as shown in Scheme 1.

Since these two mechanisms generate the same ionic product and since the detection of the distinct neutral products presents serious analytical challenges, gas-phase experiments that address this competition are severely limited.^{5,7–18} One distinguishing

Scheme 1



difference between these two mechanisms, however, is that S_N2 mechanisms generally display inverse deuterium kinetic isotope effects ($\text{KIE} < 1$), while E2 mechanisms display normal

(1) Mackay, G. I.; Bohme, D. K. *J. Am. Chem. Soc.* **1978**, *100*, 327.
 (2) Olmstead, W. N.; Brauman, J. I. *J. Am. Chem. Soc.* **1977**, *99*, 4219.
 (3) Brauman, J. I.; Blair, L. K. *J. Am. Chem. Soc.* **1970**, *92*, 5986.
 (4) Brodbelt, J. S.; Isbell, J.; Goodman, J. M.; Secor, H. V.; Seeman, J. I. *Tetrahedron Lett.* **2001**, *42*, 6949.
 (5) Villano, S. M.; Kato, S.; Bierbaum, V. M. *J. Am. Chem. Soc.* **2006**, *128*, 736.
 (6) Hu, W. P.; Truhlar, D. G. *J. Am. Chem. Soc.* **1996**, *118*, 860.
 (7) Lieder, C. A.; Brauman, J. I. *Int. J. Mass Spectrom. Ion Process.* **1975**, *16*, 307.

(8) Wladkowski, B. D.; Brauman, J. I. *J. Am. Chem. Soc.* **1992**, *114*, 10643.
 (9) Lum, R. C.; Grabowski, J. J. *J. Am. Chem. Soc.* **1988**, *110*, 8568.
 (10) Jones, M. E.; Ellison, G. B. *J. Am. Chem. Soc.* **1989**, *111*, 1645.
 (11) Gronert, S.; DePuy, C. H.; Bierbaum, V. M. *J. Am. Chem. Soc.* **1991**, *113*, 4009.
 (12) DePuy, C. H.; Gronert, S.; Mullin, A.; Bierbaum, V. M. *J. Am. Chem. Soc.* **1990**, *112*, 8650.
 (13) Gronert, S.; Pratt, L. M.; Mogali, S. *J. Am. Chem. Soc.* **2001**, *123*, 3081.
 (14) Gronert, S.; Fagin, A. E.; Okamoto, K.; Mogali, S.; Pratt, L. M. *J. Am. Chem. Soc.* **2004**, *126*, 12977.
 (15) Gronert, S. *Acc. Chem. Res.* **2003**, *36*, 848.
 (16) Lum, R. C.; Grabowski, J. J. *J. Am. Chem. Soc.* **1992**, *114*, 9663.
 (17) Noest, A. J.; Nibbering, N. M. M. *Adv. Mass Spectrom.* **1980**, *8*, 227.
 (18) Bartmess, J. E.; Hays, R. L.; Khatri, H. N.; Misra, R. N.; Wilson, S. R. *J. Am. Chem. Soc.* **1981**, *103*, 4746.

deuterium kinetic isotope effects (KIE > 1). Deuterium kinetic isotope effects are defined as the ratio of perprotio to perdeuterio rate constants (KIE = k_H/k_D). Deuteration of the neutral reactant changes the rate of the reaction, providing insight into the transition state structure and hence the reaction mechanism. The origin of these effects is primarily the result of changes in vibrational frequencies as the reaction proceeds from the reactants to the transition state structure.¹⁹ In an S_N2 reaction (Scheme 1a) an inverse KIE is due to the shortening of the C_α-H bonds in going from the reactants to the transition state; thus, the threshold energy decreases upon deuteration, $E_H^\ddagger > E_D^\ddagger$. In an E2 mechanism (Scheme 1b) the normal KIE is primarily attributed to the lengthening of the C_β-H bond in going from the reactants to transition state; thus, the threshold energy increases upon deuteration, $E_H^\ddagger < E_D^\ddagger$. When both reaction pathways are viable an overall KIE is measured, which provides qualitative insight into the competition between these two mechanisms.

We have recently measured the experimental overall reaction rate constants and deuterium KIEs for the reactions of ClO⁻ + RCl (R = methyl, ethyl, isopropyl and *tert*-butyl).⁵ This systematic approach indicates that, for the reaction of ClO⁻ with C₂H₅Cl (shown in Scheme 1), both the S_N2 and E2 channels occur, as predicted by computations of Hu and Truhlar.⁶ However, the experimental and theoretical reaction efficiencies and KIEs differ from each other, suggesting that the S_N2 channel is more prominent than calculations predict. The discrepancy between experiment and theory is mainly attributed to the inherent difficulty in accurately calculating the S_N2 and E2 barrier heights.

Nucleophiles such as ClO⁻ have been the subject of intense study for another reason. Nucleophiles of this type, where there is a lone pair of electrons on the atom that is adjacent to the nucleophilic center, have been shown to display an enhanced reactivity relative to that expected from a Bronsted-type correlation. This type of nucleophile is known as an “α-nucleophile,” and the enhanced reactivity is termed an “α-effect.”²⁰ In solution, this effect has been observed in several different types of reactions including substitution reactions.^{21–27} However, in gas-phase reactions there has been continuing controversy about whether or not the α-effect exists,^{25,28–36} prompting the question: is an α-effect actually a solvent-induced effect?

Only a limited number of gas-phase experiments have addressed this question. In an early study, DePuy et al.³⁴ found that the reactivity of HO₂⁻ was similar to that of HO⁻ in the reaction with methyl formate. These reactions proceed via three channels: proton abstraction, B_{AC}2 addition to the carbonyl center, and S_N2 substitution at the methyl group. The product branching fractions for these anions were found to be similar; thus, HO₂⁻ does not show an enhanced reactivity toward addition or substitution. In a similar approach, McAnoy et al.²⁸ have recently studied the reactions of HO₂⁻ and CD₃O⁻ with

dimethyl methylphosphonate. These reactions proceed by proton abstraction and by S_N2 substitution at a methyl group. The HO₂⁻ anion primarily reacts via substitution while the CD₃O⁻ anion preferentially reacts via proton abstraction. The difference in the reactivity of the two anions is attributed to the α-nucleophilicity of the HO₂⁻ anion. This conclusion is supported by computations, which find that the S_N2 barrier is lower (by ~1.9 kcal mol⁻¹) for the reaction of HO₂⁻. While these two studies come to conflicting conclusions, a compelling feature of the latter study is that the basicity of the HO₂⁻ and CD₃O⁻ anions are comparable; however, the absolute rate constants were not measured.

Recent theoretical work predicts that the α-effect results from an intrinsic property of a nucleophile, and therefore this effect should be manifested in the gas-phase. Ren and Yamataka^{29,30} have investigated a series of S_N2 reactions, including the reactions of ClO⁻ and BrO⁻ with methyl, ethyl, and isopropyl chloride, using G2(+) calculations. In this work, the authors plot the barrier heights for the reactions of normal nucleophiles versus basicity to obtain a linear correlation curve. The barrier heights for the reactions of the α-nucleophiles were projected onto this plot and were found to be smaller than what is predicted for a hypothetical normal nucleophile of similar basicity; thus, these results provide evidence for a gas-phase α-effect. The size of this α-effect is proportional to the amount of the deviation from the correlation curve and scales with the size of the neutral substrate and with the electronegativity of the α-atom.

In this work we report overall reaction rate constants and deuterium KIEs for the reactions of BrO⁻ with RCl, where R = methyl, ethyl, isopropyl, and *tert*-butyl. These results are consistent with the previously reported reaction rate constants and deuterium KIEs for the analogous reactions of the ClO⁻ anion,⁵ indicating that the reactions of BrO⁻ with ethyl chloride and isopropyl chloride occur by both an S_N2 and an E2 mechanism. The reactions of BrO⁻ with methyl chloride, ethyl chloride, and isopropyl chloride additionally proceed by a third reaction pathway, which was not reported in the previous ClO⁻ study. These results have prompted us to reinvestigate the products formed in the reactions of ClO⁻ with RCl. Lastly, we investigate the α-nucleophilicity of the ClO⁻ and BrO⁻ anions by comparing their reactivity to that of other nucleophiles and with the HO₂⁻ anion.

Experimental Section

These experiments were carried out using a flowing afterglow-selected ion flow tube (FA-SIFT) mass spectrometer, which previously has been described.³⁷ Reactant ions, BrO⁻ or ClO⁻, were

- (19) Poirier, R. A.; Wang, Y. L.; Westaway, K. C. *J. Am. Chem. Soc.* **1994**, *116*, 2526.
 (20) Edwards, J. O.; Pearson, R. G. *J. Am. Chem. Soc.* **1962**, *84*, 16.
 (21) Fountain, K. R.; Felkerson, C. J.; Driskell, J. D.; Lamp, B. D. *J. Org. Chem.* **2003**, *68*, 1810.
 (22) Fountain, K. R.; Hutchinson, L. K.; Mulhearn, D. C.; Xu, Y. B. *J. Org. Chem.* **1993**, *58*, 7883.
 (23) Fountain, K. R.; Taad-y, D. B.; Paul, T. W.; Golynskiy, M. V. *J. Org. Chem.* **1999**, *64*, 6547.
 (24) McIsaac, J. E.; Mulhausen, H. A.; Behrman, E. J.; Subbaram, J.; Subbaram, L. R. *J. Org. Chem.* **1972**, *37*, 1037.

- (25) Dixon, J. E.; Bruice, T. C. *J. Am. Chem. Soc.* **1971**, *93*, 6592.
 (26) Gregory, M. J.; Bruice, T. C. *J. Am. Chem. Soc.* **1967**, *89*, 4400.
 (27) Buncel, E.; Wilson, H. R.; Chuaqui, C. *J. Am. Chem. Soc.* **1982**, *1982*, 4896.
 (28) McAnoy, A. M.; Paine, M. R. L.; Blanksby, S. J. *Org. Biomol. Chem.* **2008**, *6*, 2316.
 (29) Ren, Y.; Yamataka, H. *J. Org. Chem.* **2007**, *72*, 5660.
 (30) Ren, Y.; Yamataka, H. *Chem.—Eur. J.* **2007**, *13*, 677.
 (31) Patterson, E. V.; Fountain, K. R. *J. Org. Chem.* **2006**, *71*, 8121.
 (32) Evanseck, J. D.; Blake, J. F.; Jorgensen, W. L. *J. Am. Chem. Soc.* **1987**, *109*, 2349.
 (33) Hupe, D. J.; Wu, D. *J. Am. Chem. Soc.* **1977**, *99*, 7653.
 (34) DePuy, C. H.; Della, E. W.; Filley, J.; Grabowski, J. J.; Bierbaum, V. M. *J. Am. Chem. Soc.* **1983**, *105*, 2481.
 (35) Buncel, E.; Um, I.-H. *Tetrahedron* **2004**, *60*, 7801.
 (36) Hoz, S. *J. Org. Chem.* **1982**, *47*, 3545.
 (37) Van Doren, J. M.; Barlow, S. E.; DePuy, C. H.; Bierbaum, V. M. *Int. J. Mass Spectrom. Ion Process.* **1987**, *81*, 85.

Table 1. Reaction Rate Constants ($10^{-10} \text{ cm}^3 \text{ s}^{-1}$), Kinetic Isotope Effects, and Product Ion Branching Fractions for the Reactions of $^{79}\text{BrO}^-$ and $^{35}\text{ClO}^-$ with RCl ($\text{R} = \text{methyl, ethyl, iso-propyl, and } tert\text{-butyl}$)

reaction	k^c	KIE	ionic products	branching fractions
$^{79}\text{BrO}^- + \text{CH}_3\text{Cl}^a$	1.08 ± 0.03		Cl^- , $^{79}\text{Br}^-$	0.82, 0.18
$^{79}\text{BrO}^- + \text{CD}_3\text{Cl}^a$	1.31 ± 0.04	0.82 ± 0.03	Cl^- , $^{79}\text{Br}^-$	0.86, 0.14
$^{79}\text{BrO}^- + \text{CH}_3\text{CH}_2\text{Cl}^a$	1.07 ± 0.01		Cl^- , $^{79}\text{Br}^-$	0.91, 0.09
$^{79}\text{BrO}^- + \text{CD}_3\text{CD}_2\text{Cl}^a$	1.11 ± 0.03	0.96 ± 0.03	Cl^- , $^{79}\text{Br}^-$	0.92, 0.08
$^{79}\text{BrO}^- + \text{CH}_3\text{CD}_2\text{Cl}^a$	1.12 ± 0.02	0.95 ± 0.02	Cl^- , $^{79}\text{Br}^-$	0.93, 0.07
$^{79}\text{BrO}^- + \text{CD}_3\text{CH}_2\text{Cl}^a$	1.05 ± 0.04	1.02 ± 0.04	Cl^- , $^{79}\text{Br}^-$	0.91, 0.09
$^{79}\text{BrO}^- + (\text{CH}_3)_2\text{CHCl}^{a,d}$	0.934 ± 0.016		Cl^- , $^{79}\text{Br}^-$, $\text{Cl}^- (\text{HO}^{79}\text{Br})$	0.97, 0.03, trace
$^{79}\text{BrO}^- + (\text{CD}_3)_2\text{CDCl}^{a,d}$	0.352 ± 0.014	2.65 ± 0.11	Cl^- , $^{79}\text{Br}^-$, $\text{Cl}^- (\text{DO}^{79}\text{Br})$	0.92, 0.08, trace
$^{79}\text{BrO}^- + (\text{CH}_3)_3\text{CCl}^{a,e}$	1.93 ± 0.11		Cl^- , $\text{Cl}^- (\text{HO}^{79}\text{Br})$	1.00, trace
$^{79}\text{BrO}^- + (\text{CD}_3)_3\text{CCl}^{a,e}$	0.638 ± 0.023	3.03 ± 0.22	Cl^- , $\text{Cl}^- (\text{DO}^{79}\text{Br})$	1.00, trace
$^{35}\text{ClO}^- + \text{CH}_3\text{Cl}^b$	2.01 ± 0.01		Cl^- , $^{35}\text{Cl}^-$	0.73, 0.27
$^{35}\text{ClO}^- + \text{CD}_3\text{Cl}^b$	2.36 ± 0.01	0.85 ± 0.01	Cl^- , $^{35}\text{Cl}^-$	0.78, 0.22
$^{35}\text{ClO}^- + \text{CH}_3\text{CH}_2\text{Cl}^b$	2.25 ± 0.01		Cl^- , $^{35}\text{Cl}^-$	0.90, 0.10
$^{35}\text{ClO}^- + \text{CD}_3\text{CD}_2\text{Cl}^b$	2.27 ± 0.01	0.99 ± 0.01	Cl^- , $^{35}\text{Cl}^-$	0.90, 0.10
$^{35}\text{ClO}^- + \text{CH}_3\text{CD}_2\text{Cl}^a$	2.35 ± 0.01	0.96 ± 0.01	Cl^- , $^{35}\text{Cl}^-$	0.90, 0.10
$^{35}\text{ClO}^- + \text{CD}_3\text{CH}_2\text{Cl}^a$	2.17 ± 0.02	1.04 ± 0.01	Cl^- , $^{35}\text{Cl}^-$	0.89, 0.11
$^{35}\text{ClO}^- + (\text{CH}_3)_2\text{CHCl}^{b,d}$	1.74 ± 0.03		Cl^- , $^{35}\text{Cl}^-$	0.94, 0.06
$^{35}\text{ClO}^- + (\text{CD}_3)_2\text{CDCl}^{b,d}$	1.01 ± 0.02	1.71 ± 0.05	Cl^- , $^{35}\text{Cl}^-$	0.90, 0.10
$^{35}\text{ClO}^- + (\text{CH}_3)_3\text{CCl}^{b,d}$	2.33 ± 0.03		Cl^-	1.00
$^{35}\text{ClO}^- + (\text{CD}_3)_3\text{CCl}^{b,d}$	1.01 ± 0.05	2.31 ± 0.12	Cl^-	1.00

^a This work. ^b Reaction rate constants and KIEs are from ref 5; branching ratios determined in this work. ^c The error is the standard deviation of at least three measurements. ^d A negligible amount of an association product was observed. ^e An association channel of 0.01 for the perprotio reaction and 0.04 for the perdeuterio reaction was observed; this component was removed from the overall reaction rate constant.

formed in the source flow tube from electron impact on N_2O to produce O^- , which was then allowed to react with CCl_3Br or CCl_4 , respectively. Ions of a single isotopomer, $^{35}\text{ClO}^-$ and $^{79}\text{BrO}^-$, were mass selected by a quadrupole mass filter and injected into the reaction flow tube where they are thermalized to $302 \pm 2 \text{ K}$ by collisions with He buffer gas ($\sim 0.5 \text{ Torr}$, 10^4 cm s^{-1}). Despite injecting the reactant ions with minimal energy, $^{79}\text{Br}^-$ or $^{35}\text{Cl}^-$ ions produced from the collision-induced dissociation of the parent ion were also present in the reaction flow tube; the presence of these additional ions was considered in the data analysis below.

Measured flows of neutral reagents were introduced into the reaction flow tube through a series of fixed inlets along the reaction flow tube, and the reactant and product ions were analyzed by a quadrupole mass filter coupled to an electron multiplier. Neutral reactant flow rates were measured by monitoring the pressure change versus time in a calibrated volume system. Reaction rate constants and product branching ratios were determined by varying the position at which neutral reagents were added, thereby changing the reaction distance and time, while monitoring the change in reactant ion intensity. The ratio of perprotio to perdeuterio rate constants gives the KIE ($\text{KIE} = k_{\text{H}}/k_{\text{D}}$). Product branching ratios were determined by plotting the percentage of each ion at each neutral inlet; extrapolation to “zero distance” gives the branching ratio. Efforts were made to minimize mass discrimination; however, it was necessary to estimate the relative detection sensitivities when calculating product ion branching ratios. The relative detection sensitivity was estimated by examining a series of exothermic ion–molecule reactions where only one ionic product was formed.

The error reported for the reaction rate constants is one standard deviation of at least three measurements. The systematic error associated with an individual rate constant is $\pm 20\%$; however, the KIEs are more accurately determined because some of the systematic errors (pressure, temperature, He flow rate, etc.) cancel in the rate constant ratio. The estimated error in the product branching fractions is $\pm 25\%$ of the smaller product channel; this is mostly attributed to mass discrimination and to the fact that X^- results both from collision-induced dissociation (CID) of the reactant ion and from the reaction. Helium buffer gas (99.995%) was purified by passage through a liquid nitrogen cooled molecular sieve trap. Neutral reagents were purchased from commercial sources and used

without further purification.³⁸ However, it was verified that HCl was not a significant contaminant by mass selecting $^{35}\text{Cl}^-$ and allowing it to react with the neutral reagents. It has previously been shown that the reaction rates of Cl^- with these alkyl halides are below the detection limits of our instrument, while the Cl^- with HCl exchange reaction proceeds at approximately half of the collision rate.³⁹ Thus, the absence of $^{37}\text{Cl}^-$ as a product ion demonstrates that HCl is not a significant contaminant. An HCl impurity would complicate the rate measurements due to a rapid proton transfer pathway, which could not be distinguished from the $\text{S}_{\text{N}}2$ and E2 channels.

Optimized geometries and harmonic vibrational frequencies (unscaled) for the reactants, products, and transition state structures were determined from electronic structure calculations using the Gaussian 03 suite of programs⁴⁰ at the MP2(FC)/aug-cc-pVDZ level of theory.^{41,42} Transition state structures were identified to have only one imaginary frequency, and this frequency was animated to verify that its motion corresponds to the transition state reaction coordinate. Optimized geometries, energies, and frequencies for the reactants, products, and transition state structures are provided in the Supporting Information.

Results and Discussion

The experimental reaction rate constants, product branching fractions, and deuterium kinetic isotope effects are reported in Table 1 for the reactions of BrO^- with RCl ($\text{R} = \text{methyl, ethyl, isopropyl, and } tert\text{-butyl}$, abbreviated as Me, Et, *i*-Pr, and *t*-Bu). These results are consistent with the reaction rate constants and KIEs for the reactions of ClO^- with RCl ,⁵ also shown in Table 1. For a given neutral reagent, the reactions of BrO^- are slightly less efficient than those of ClO^- and the kinetic isotope effects

(38) CH_3Cl 99.9%, CD_3Cl 99% D, $\text{C}_2\text{H}_5\text{Cl} \geq 99\%$, $\text{C}_2\text{D}_5\text{Cl}$ 99.6% D, $\text{CD}_3\text{CH}_2\text{Cl}$ 99.7% D, $\text{CH}_3\text{CD}_2\text{Cl}$ 99.1% D, *i*- $\text{C}_3\text{H}_7\text{Cl} \geq 99\%$, *i*- $\text{C}_3\text{D}_7\text{Cl}$ 98% D, *t*- $\text{C}_4\text{H}_9\text{Cl} \geq 99\%$, *t*- $\text{C}_4\text{D}_9\text{Cl}$ 99% D.

(39) Van Doren, J. M.; DePuy, C. H.; Bierbaum, V. M. *J. Phys. Chem.* **1989**, *93*, 1130.

(40) Frisch, M. J.; Trucks, G. W.; Schlegel, H. B.; Scuseria, G. E.; Robb, M. A.; et al. Gaussian 03, revision B.05, Gaussian, Inc.: Pittsburgh, PA, 2003.

(41) Hehre, W. J.; Radom, L.; Schleyer, P. v. R.; Pople, J. A. *Ab Initio Molecular Orbital Theory*; Wiley: New York, 1986.

(42) Woon, D. E.; Dunning, T. H. *J. Chem. Phys.* **1993**, *98*, 1358.

become more pronounced. This trend reflects the weaker basicity of the BrO^- anion ($353.5 \text{ kcal mol}^{-1}$) relative to the ClO^- anion ($355.6 \text{ kcal mol}^{-1}$).

Both an $\text{S}_{\text{N}}2$ mechanism and an E2 mechanism result in the formation of Cl^- , which is the major product formed in each reaction. The reactions of BrO^- with MeCl , EtCl , and $i\text{-PrCl}$ also produce minor amounts of Br^- ; this product was not observed for the reaction of BrO^- with $t\text{-BuCl}$. Additionally, the reactions of BrO^- with $i\text{-PrCl}$ and $t\text{-BuCl}$ produce trace amounts (<1%) of an E2 product cluster, $\text{Cl}^-(\text{BrOH})$ or $\text{Cl}^-(\text{BrOD})$, and minor amounts of an association product, $\text{BrO}^-(\text{RCl})$. For the reaction with $i\text{-PrCl}$, the amount of association that occurs is negligibly small. For the reaction with $t\text{-BuCl}$, the association channel is less than 5% of the total reaction; this contribution is removed from the rate constants and KIEs in Table 1.

The formation of Br^- from the reactions of BrO^- with MeCl , EtCl , and $i\text{-PrCl}$ is rather unexpected and has prompted us to reinvestigate the corresponding reactions of ClO^- . For these reactions, a prototypical $\text{S}_{\text{N}}2$ or E2 process results in the formation of Cl^- with an isotope distribution that reflects the natural Cl atom abundance in RCl (76:24). However, for the reactions of ClO^- with MeCl , EtCl , and $i\text{-PrCl}$, the Cl^- isotope distribution is skewed slightly toward the $^{35}\text{ClO}^-$ reactant ion isotopomers. For the reaction of ClO^- with $t\text{-BuCl}$, the Cl^- isotope distribution reflects that of the natural abundance of Cl in $t\text{-BuCl}$. This additional pathway had previously gone unnoticed since CID of the $^{35}\text{ClO}^-$ reactant ion upon SIFT-injection results in the formation of $^{35}\text{Cl}^-$. The presence of this fragment ion results in the appearance of a skewed $^{35}\text{Cl}/^{37}\text{Cl}$ isotope distribution. However, by subtracting the amount of initial $^{35}\text{Cl}^-$ due to CID from the product distribution, we were able to determine the product ion $^{35}\text{Cl}/^{37}\text{Cl}$ isotope distribution; the deviation from the Cl natural abundance gives the branching ratio for the two pathways (Table 1).

For both anions, the occurrence of this additional reaction pathway is most significant for the reaction with MeCl and gradually diminishes as the size of the neutral substrate increases. This trend correlates with the anticipated falloff of the $\text{S}_{\text{N}}2$ channel as steric factors become more important, suggesting that this additional product channel may result from a transformation within the $\text{S}_{\text{N}}2$ product ion-dipole complex. It is well established that $\text{S}_{\text{N}}2$ reactions are characterized by a double well potential energy surface, where two stable ion-dipole complexes flank the transition state.² Depending on the thermodynamics of the system, the lifetime of these complexes can be relatively long, allowing for additional chemistry to occur.⁴³ The complex retains all of its initial energy since there are no collisions during its lifetime; thus, endothermic processes can be driven by the complexation energy, and as long as the overall process is exothermic, the complex can dissociate into products.

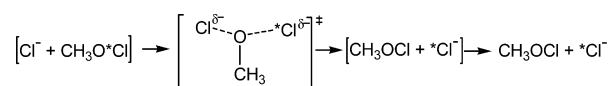
- (43) DePuy, C. H.; Bierbaum, V. M. *J. Am. Chem. Soc.* **1981**, *103*, 5034.
 (44) King, G. K.; Maricq, M. M.; Bierbaum, V. M.; DePuy, C. H. *J. Am. Chem. Soc.* **1981**, *103*, 7133.
 (45) Kato, S.; Davico, G. E.; Lee, H. S.; DePuy, C. H.; Bierbaum, V. M. *Int. J. Mass Spectrom.* **2001**, *210*, 223.
 (46) Viggiano, A. A.; Morris, R. A.; Paschkewitz, J. S.; Paulsen, J. F. *J. Am. Chem. Soc.* **1992**, *114*, 10477.
 (47) Su, T.; Chesnavich, W. J. *J. Chem. Phys.* **1982**, *76*, 5183.
 (48) Grabowski, J. J. Studies of Gas Phase Ion-Molecule Reactions Using a Selected Ion Flow Tube. Ph.D. Thesis, University of Colorado at Boulder, 1983.
 (49) Tanaka, K.; Mackay, G. I.; Payzant, J. D.; Bohme, D. K. *Can. J. Chem.* **1976**, *54*, 1643.
 (50) Ren, Y.; Yamataka, H. *Org. Lett.* **2005**, *8*, 119.

Table 2. Reaction Exothermicities^a (kcal mol^{-1}) for the Reactions of BrO^- and ClO^- with RCl (R = methyl, ethyl, iso-propyl, and *tert*-butyl)

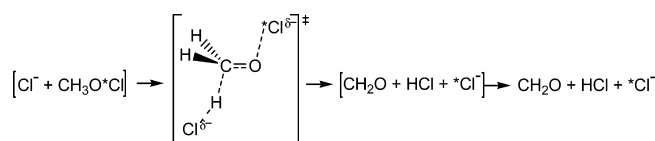
reaction	E2 ^b	$\text{S}_{\text{N}}2^c$	$\text{S}_{\text{N}}2$ -induced substitution ^d	$\text{S}_{\text{N}}2$ -induced elimination ^e
$\text{BrO}^- + \text{CH}_3\text{Cl}$	n/a	-21 ^f	-23	-59
$\text{BrO}^- + \text{CH}_3\text{CH}_2\text{Cl}$	-4	-23 ^f	-25	-69
$\text{BrO}^- + (\text{CH}_3)_2\text{CHCl}$	-5	-23 ^f	-25	-66
$\text{BrO}^- + (\text{CH}_3)_3\text{CCl}$	-4	-24 ^f	-26	n/a
$\text{ClO}^- + \text{CH}_3\text{Cl}$	n/a	-20	-20	-56
$\text{ClO}^- + \text{CH}_3\text{CH}_2\text{Cl}$	-6	-22	-22	-66
$\text{ClO}^- + (\text{CH}_3)_2\text{CHCl}$	-6	-22	-22	-69
$\text{ClO}^- + (\text{CH}_3)_3\text{CCl}$	-6	-23	-23	n/a

^a Enthalpies of formation are determined from the thermochemical data on the NIST WebBook⁵¹ or from the JANAF thermochemical tables.⁵² ^b See Scheme 1b. The formation of the E2 cluster is not considered. ^c See Scheme 1a. ^d See Scheme 2. ^e See Scheme 3. ^f Enthalpy of formation of CH_3OBr is calculated in ref 53; for $\text{C}_2\text{H}_5\text{OBr}$, $\text{C}_3\text{H}_7\text{OBr}$, and $\text{C}_4\text{H}_9\text{OBr}$, enthalpies of formation are estimated.

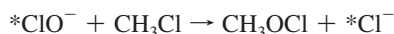
Scheme 2



Scheme 3



A possible reaction that would account for the formation of these products is shown in eq 1 for the reactions of ClO^- with CH_3Cl ; the Cl atom that originates from ClO^- is indicated with an asterisk.



$$\Delta H_{\text{rxn}} = -20 \text{ kcal mol}^{-1} \quad (1)$$

This reaction presumably is initiated by the $\text{S}_{\text{N}}2$ reaction of $*\text{ClO}^- + \text{CH}_3\text{Cl}$, where $*\text{ClO}^-$ attacks the carbon atom of methyl chloride to displace Cl^- (analogous to Scheme 1a). A second substitution step within the $[\text{Cl}^- + \text{CH}_3\text{O}^*\text{Cl}]$ ion-dipole complex, would scramble the chlorine atoms. This second substitution reaction presumably would proceed in a concerted step, as shown Scheme 2, where Cl^- attacks the oxygen atom of $\text{CH}_3\text{O}^*\text{Cl}$ displacing $*\text{Cl}^-$. For the reaction of the ClO^- anion, this mechanism produces the same products as the traditional $\text{S}_{\text{N}}2$ reaction; however, the chlorine atoms are exchanged in a thermoneutral process. For the reactions of the BrO^- anion, a substitution step that exchanges Cl for Br is slightly more exothermic. These exothermicities ($\text{S}_{\text{N}}2$ -induced substitution) are summarized in Table 2.

A second possible reaction that would account for the formation of these products is shown in eq 2. These exother-

- (51) Linstrom, P. J.; Mallard, W. G. NIST Chemistry WebBook, NIST Standard Reference Database Number 69. National Institute of Standards and Technology, Gaithersburg, MD; June 2005.
 (52) Chase, W. M., Jr.; Davies, C. A.; Downey, J. J. R.; Frurip, D. J.; McDonald, R. A.; Syverud, A. N. JANAF Thermochemical Tables, 3rd ed., Parts I and II. *J. Phys. Chem. Ref. Data*, 1985; Suppl 1.
 (53) Espinosa-Garcia, J. *Chem. Phys. Lett.* **1999**, *315*, 239.
 (54) Unpublished Results: $k = 7.50 \times 10^{-10} \text{ cm}^3 \text{ s}^{-1}$ for $\text{CFH}_2\text{CH}_2\text{O}^- + \text{CH}_3\text{Cl}$ and $k = 4.28 \times 10^{-10} \text{ cm}^3 \text{ s}^{-1}$ for $\text{CF}_2\text{HCH}_2\text{O}^- + \text{CH}_3\text{Cl}$.
 (55) Bohme, D. K.; Young, L. B. *J. Am. Chem. Soc.* **1970**, *92*, 7354.

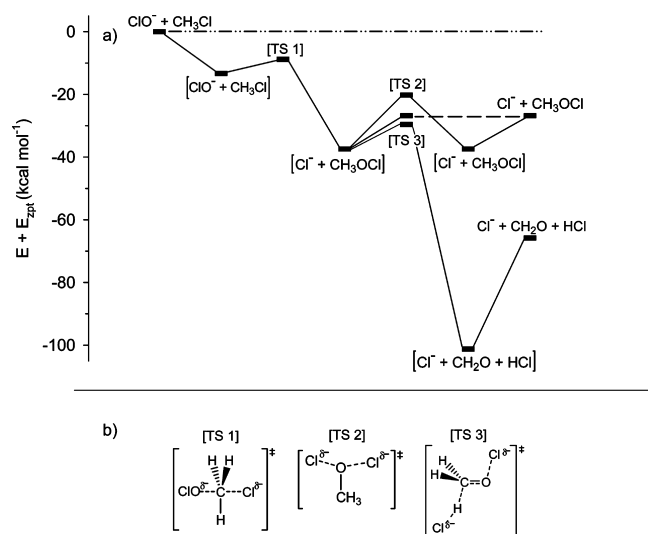
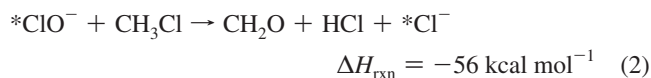


Figure 1. (a) Reaction coordinate diagram for the reaction of ClO^- with CH_3Cl . The relative energies (electronic + zero point energy) were calculated at the MP2/aug-cc-pVDZ level of theory; (b) the transition state structures are provided.

micities ($\text{S}_{\text{N}}2$ -induced elimination) are also summarized in Table 2.



This reaction is consistent with an elimination reaction that occurs following the initial substitution step, within the $\text{S}_{\text{N}}2$ product ion-dipole complex as shown in Scheme 3. This second transformation likely occurs in a concerted step where Cl^- abstracts an H atom from $\text{CH}_3\text{O}^*\text{Cl}$, displacing $*\text{Cl}^-$ and forming a C–O double bond; similar elimination reactions have previously been reported for alkyl nitrites.^{17,44} The transition state for this reaction resembles that of a typical E2 transition state, where the two leaving groups are antiperiplanar to one another.

Because we cannot detect the neutral products we are not able to distinguish between these two proposed mechanisms. Electronic structure calculations were employed to explore whether or not these two potential mechanisms are thermodynamically feasible. These results are summarized in Figure 1 for the reaction of ClO^- with CH_3Cl . For both possible reactions, the highest energy point is the first $\text{S}_{\text{N}}2$ barrier, TS1; passage over this barrier is the rate-limiting step. If the reaction occurs according to Scheme 2, the reaction proceeds through TS2 into a second product ion-dipole well. Passage over the second substitution barrier requires more energy than for the initial $\text{S}_{\text{N}}2$ products to separate. If the reaction occurs according to Scheme 3, the reaction proceeds through TS3. This elimination barrier is below the second substitution barrier (TS2) and below the energy required for the initial $\text{S}_{\text{N}}2$ products to separate. While both proposed mechanisms are thermodynamically viable, the $\text{S}_{\text{N}}2$ -induced elimination channel (Scheme 3) is energetically more feasible, and the overall reaction is considerably more exothermic. Moreover, the occurrence of a second elimination step is favored dynamically since passage over the first substitution barrier (TS1) leads to an $\text{S}_{\text{N}}2$ product ion-dipole complex where the displaced Cl^- anion is positioned behind the CH_3OCl methyl group. Thus, the Cl^- anion can readily abstract a hydrogen atom as in Scheme 3, whereas nucleophilic

attack on the oxygen atom as in Scheme 2 requires the anion to maneuver around the methyl group.

A similar computational study was done for the reaction of BrO^- with CH_3Cl . In this case, the relative energetics for the substitution–elimination pathway were found to be similar to the corresponding reaction of ClO^- . However, for this reaction we were unable to locate a saddle point corresponding to the second substitution transition state, TS2. This provides additional support for the occurrence of the $\text{S}_{\text{N}}2$ -induced elimination mechanism rather than the double substitution mechanism. However, without performing a more exhaustive theoretical investigation, which is beyond the scope of this work, we cannot state with certainty which mechanism is responsible for this additional channel.

Kinetic Isotope Effects. For a given neutral reagent, the reactions of BrO^- with RCl are less efficient than those of ClO^- with RCl and, as the reaction efficiency decreases, the magnitude (deviation from unity) of the KIE increases. The efficiencies of these reactions are all well below the collision-controlled limit; therefore, the KIE is expected to accurately reflect the transition state. The larger isotope effects observed for the reactions of BrO^- with RCl are consistent with variational transition state theory, where less exothermic reactions have later transition states, which more closely resemble the geometry where the maximum isotope effect is expected. As a point of clarification, when the magnitude of a KIE is discussed as large or small, this refers to the absolute value of the displacement from unity. The terms inverse and normal indicate whether the KIE is less than one or greater than one, respectively.

With both sets of reactions, the KIE becomes increasingly more normal as the size of the alkyl substrate increases. These results indicate that the E2 pathway becomes the dominant channel as the neutral reagent becomes more sterically hindered. The reactions with *t*-BuCl are expected to exclusively occur via an E2 mechanism. Previous results have shown that the sterically bulky *tert*-butyl group inhibits the $\text{S}_{\text{N}}2$ pathway.¹² The normal effect observed for these reactions is consistent with other E2 isotope effects reported in the literature.¹¹

The reactions of MeCl proceed by two pathways; for the remainder of this discussion, the major, prototypical $\text{S}_{\text{N}}2$ substitution channel will be referred to as the “direct substitution” channel and the minor channel will be referred to as the “substitution-induced displacement” channel. Since the rate-limiting step in both pathways is crossing the initial $\text{S}_{\text{N}}2$ barrier (Figure 1), the KIEs for these reactions are exclusively attributed to the $\text{S}_{\text{N}}2$ mechanism. The inverse KIEs measured for these reactions are consistent with the KIEs of other $\text{S}_{\text{N}}2$ reactions reported in the literature.^{45,46} For a given anion reacting with a perprotio and perdeuterio alkyl chloride, the substitution-induced displacement product branching fraction is larger for the slower reaction. For example, in the reaction of BrO^- with MeCl , the perprotio reaction is slower but shows a larger fraction of secondary reaction (0.18) within the product complex relative to the perdeuterio compound (0.14). The change in branching fraction with overall reactivity is most likely due to dynamical factors within the $\text{S}_{\text{N}}2$ -product ion-dipole complex.

The KIEs measured for the reactions of EtCl and *i*-PrCl are larger than the KIEs measured in the MeCl reactions but smaller than the KIEs measured for the *t*-BuCl reactions, indicating that these reactions proceed by competing $\text{S}_{\text{N}}2$ and E2 mechanisms. For these reactions, the substitution-induced displacement channel is small. However, the occurrence of this mechanism provides evidence that these reactions proceed partially by an

S_N2 mechanism, since this channel results from a second reaction step within the S_N2 product ion-dipole complex. The reaction of BrO^- with *i*-PrCl additionally produces trace amounts of a clustered product, $\text{Cl}^-(\text{HOBr})$, providing evidence that this reaction proceeds partially through an elimination mechanism since HOBr is a neutral product of this mechanism. This E2 cluster is also observed for the reaction of BrO^- with *t*-BuCl. For these larger systems the formation of this cluster is likely promoted by the additional degrees of freedom, hence a longer lifetime of the product ion-dipole complex.

To further verify that the EtCl systems proceed by both an S_N2 and an E2 mechanism, we have measured kinetic isotope effects that arise from the selective deuteration at the α and β positions of the EtCl (termed *d*2-KIE and *d*3-KIE, respectively). The *d*2-KIEs are slightly more inverse than the *d*5-KIEs, consistent with the occurrence of an S_N2 mechanism. Deuteration at the α -position is expected to be more sensitive to the S_N2 pathway since the inverse effect is predominantly the result of changes in the $\text{C}_\alpha\text{-H}$ vibrational modes. The *d*3-KIEs are slightly more normal than the *d*5-KIEs, reflecting the occurrence of an E2 mechanism. Deuteration at the β -position is expected to be more sensitive to the E2 pathway since the normal effect is mainly the result of changes in the $\text{C}_\beta\text{-H}$ stretching frequency. These results indicate that both mechanisms do indeed occur. While the *d*2- and *d*3-effects provide a more sensitive probe of the S_N2 and E2 pathways, respectively, they are still an overall effect and do not reflect the absolute magnitude of the KIEs for the respective pathways.

For each anion series, the trend in the KIEs indicates that the E2 channel becomes more important for larger systems, where steric effects inhibit the S_N2 channel. In a *crude* approximation, the E2 branching fraction (BR) for the reactions of EtCl and *i*-PrCl can be estimated by assuming that the E2-KIE for these reactions is approximately equal to the KIE observed in the *t*-BuCl systems and that the S_N2 -KIE is approximately equal to the KIE observed for the MeCl system when scaled for number of α -hydrogen atoms. The total kinetic isotope effect is given by $\text{KIE}_{\text{tot}} = \text{KIE}_{\text{E2}} \times \text{BR}_{\text{E2}} + \text{KIE}_{\text{SN2}} \times \text{BR}_{\text{SN2}}$ and $\text{BR}_{\text{E2}} + \text{BR}_{\text{SN2}} = 1$, where BR_{SN2} is the combined substitution channels. The KIE for the *t*-BuCl system is not scaled for the number of hydrogen atoms, since to a first-order approximation only one $\text{C}_\beta\text{-H}$ bond is elongated in the E2 transition state (see Scheme 1b). This analysis, of course, relies on many assumptions and is only intended to provide an estimate of which pathway is dominant. For the reaction of BrO^- with EtCl, the overall KIE is 0.96. If the E2-KIE and S_N2 -KIE are taken to be 3.03 and 0.88, respectively, then the E2 channel only accounts for $\sim 5\%$ of the reaction and the combined substitution channels account for $\sim 95\%$ of the total reaction. Applying this same analysis to the reaction of ClO^- with EtCl, the E2 channel again represents only $\sim 5\%$ of the reaction. In contrast, about 80% of the reaction of BrO^- with *i*-PrCl proceeds by the E2 channel, while $\sim 60\%$ reaction of ClO^- with *i*-PrCl proceeds by the E2 channel. While this analysis is qualitative in nature, it does identify the major and minor channels.

α -Nucleophilic Character. Both BrO^- and ClO^- are prototypical α -nucleophiles. Nucleophilicity is the ability of an ion to donate a pair of electrons to an electrophile to assist displacement of a leaving group. It has been shown that in solution α -nucleophiles display an enhanced reactivity relative to that expected from a Bronsted-type correlation, which

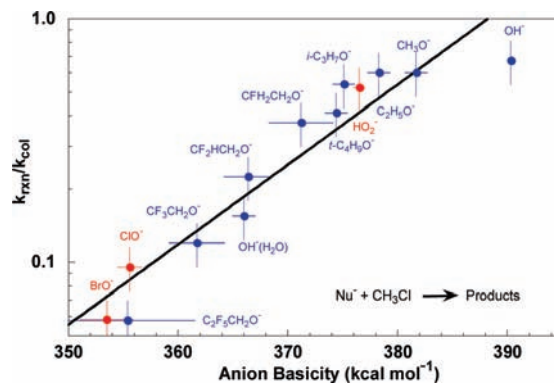


Figure 2. The log of reaction efficiency ($k_{\text{txn}}/k_{\text{col}}$) versus the anion basicity (ΔH_{298}) for the S_N2 reactions of Nu^- with CH_3Cl . The normal nucleophiles are indicated in blue and the α -nucleophiles are indicated in red. The linear trend line (black line) is fit to the normal nucleophile data set ($y = 0.0328x - 12.74$; $r^2 = 0.87$). The vertical error bars represent the absolute uncertainty of $\pm 20\%$. Reactivities: refs 12, 54, and 55; anion basicities: ref 51. We have also calculated the gas-phase basicities of these anions, and in each case the calculation is in good agreement with the experimental value. These values are provided in the Supporting Information.

relates this kinetic property to a thermodynamic property of the nucleophile. Such a correlation is shown in Figure 2, which is a plot of the log reaction efficiency ($k_{\text{txn}}/k_{\text{col}}$, where k_{col} is calculated using parametrized trajectory theory⁴⁷) as a function of anion basicity over a 40 kcal mol^{-1} range for the S_N2 reactions of various oxy-anions with CH_3Cl . The general trend displayed by the normal nucleophiles (blue circles) is that the log of reaction efficiency increases linearly with anion basicity. Unfortunately, there are few oxy-anions in the lower basicity range of ClO^- and BrO^- (red circles) whose reactions with CH_3Cl have been reported. However, by fitting a linear trend line to this data set (blue circles), the efficiency of normal nucleophiles in this lower basicity region can be estimated. The correlation coefficient (r^2) for this fit is 0.87, which is quite good considering that these two variables are not rigorously linked by a rate-energy rule (such as, for example the Arrhenius equation or statistical rate theory). The reaction efficiencies of the α -nucleophiles, ClO^- and BrO^- , are consistent with the predictions of the basicity–reactivity correlation. In fact, the trend line predicts the reaction efficiency for the ClO^- anion within the error bar of its measurement, while the measured reaction efficiency for the BrO^- anion is less than that predicted by the trend line. This is in contrast to G2(+) calculations, which predict the barriers for the reactions of BrO^- and ClO^- with CH_3Cl to be 2.5 and 3.8 kcal mol^{-1} lower than those of normal nucleophiles of comparable basicity, respectively.²⁹ On the basis of these results, we would expect the reaction efficiency of the BrO^- and ClO^- anions to be enhanced by an order of magnitude.

It perhaps can be argued that the BrO^- and ClO^- anions are poor α -nucleophiles, since the halogen–oxygen bond is relatively long, resulting in poor orbital overlap of the lone pairs on the halogen and oxygen atoms. We, therefore, have additionally studied the reaction of HO_2^- with CH_3Cl ($k = 1.23 \times 10^{-9} \text{ cm}^3 \text{ s}^{-1}$; $\text{eff} = 0.517$); this result is also included in Figure 2. The HO_2^- anion is an excellent α -nucleophile whose reactivity has been extensively studied in solution. In one study, HO_2^- was found to undergo S_N2 substitution on a methyl group ten times faster than HO^- , despite the greater basicity of the HO^- anion.²⁷ In the gas-phase, however, this anion does not display enhanced reactivity with CH_3Cl .

Again, the reaction efficiency predicted by the trend line is in good agreement with the measured reaction efficiency for this anion. In further support of these findings, the S_N2 reaction of HO_2^- with CH_3F ($k = 6.0 \times 10^{-12} \text{ cm}^3 \text{ s}^{-1}$; $\text{eff} = 0.0025$)⁴⁸ is slower than that of HO^- and CH_3O^- ($k = 2.5 \times 10^{-11} \text{ cm}^3 \text{ s}^{-1}$; $\text{eff} = 0.0087$ and $k = 1.4 \times 10^{-11} \text{ cm}^3 \text{ s}^{-1}$; $\text{eff} = 0.0058$, respectively).⁴⁹ Since these reactions proceed at rates well below the collision rate, the α -effect would be more apparent. However, the rates of these reactions scale with anion basicity and are inconsistent with a gas-phase α -effect.

This result also contradicts theoretical results, which predict that the barrier for the reaction of HO_2^- with CH_3Cl is lower (by $\sim 5.4 \text{ kcal mol}^{-1}$) than that of a nucleophile of similar basicity.⁵⁰ It is difficult to account for the discrepancies between experiment and theory. However, it is possible that these nucleophiles have different entropic factors, which would influence their reactivity. Additionally, our results disagree with the experimental findings of McAnoy et al.,²⁸ which find a larger propensity for the reaction of HO_2^- with dimethyl methylphosphonate to proceed via an S_N2 substitution rather than proton transfer, whereas the corresponding reaction of CD_3O^- proceeds primarily by proton transfer. The difference in the product branching fractions was attributed to the α -nucleophilicity of HO_2^- . In this study, however, the overall reaction rate constants for HO_2^- and CD_3O^- with dimethyl methylphosphonate could not be evaluated, and therefore it is not known if the overall reaction rates for the two reactions are comparable.

These results cast serious doubt on the existence of a gas-phase α -effect. This instead implies that the α -effect is not due to an intrinsic property of the anion but is rather due to a solvent effect. These findings are complemented by the solution studies of Um and Bunce,³⁵ which demonstrate the important and complicated role of the solvent in the destabilization/stabilization of the α -nucleophile and the transition state. However, as stated above, the calculations of Ren and Yamataka²⁹ predict that the α -effect in S_N2 reactions becomes more pronounced as the size of the neutral substrates increases. Unfortunately, given the limitations of gas-phase experiments, a similar analysis for the S_N2 reactions of larger alkyl halides (EtCl and *i*-PrCl) is not feasible since the E2 pathway is competitive. Additionally, further investigation of the gas-phase reactivity of α -nucleo-

philes with sp^2 -hybridized carbon centers is a clear target for future studies.

Conclusions

The competition between S_N2 and E2 channels for the reactions of BrO^- and ClO^- with RCl (R = methyl, ethyl, isopropyl, and *tert*-butyl) was explored through deuterium kinetic isotope effect measurements. These kinetic isotope effects become increasingly more normal as the extent of substitution in the neutral reactants increases. This indicates that the E2 channel becomes the dominant pathway as the neutral reagent becomes more sterically hindered. For the reactions of ethyl chloride, elimination is estimated to be a minor channel, while for the reactions of isopropyl chloride, elimination is estimated to be the major channel. The reactions of MeCl, EtCl, and *i*-PrCl proceed by an additional minor reaction pathway, which is likely due to a novel elimination step that occurs within the S_N2 product ion-dipole complex.

Additionally, the gas-phase substitution reactions of ClO^- and BrO^- with CH_3Cl occur as predicted by a basicity-reactivity relationship. The same result is observed for the S_N2 reaction of HO_2^- with CH_3Cl and CH_3F . The lack of enhanced reactivity of these α -nucleophiles implies that the α -effect is not manifested in the gas-phase but instead is due to a solvent effect.

Acknowledgment. We gratefully acknowledge Prof. Charles H. DePuy and Prof. Stephen J. Blanksby for their insightful comments. This work was supported by the AFOSR (FA9550-06-1-006) and NSF (CHE-0647088). The computational results are based upon work supported by the National Science Foundation under the following NSF programs: Partnerships for Advanced Computational Infrastructure, Distributed Terascale Facility (DTF) and Terascale Extensions: Enhancements to the Extensible Terascale Facility.

Supporting Information Available: The optimized geometries for the stationary points in Figure 1 are provided in Table S1. The anion basicities (both experimental and G3 calculated), reaction rate constants, and collision rate constants used in Figure 2 are provided in Table S2. Additionally the full citation to ref 40 is provided. This material is available free of charge via the Internet at <http://pubs.acs.org>.

JA9012084